IEEE Access
Multidisciplinary ⋮ Rapid Review ⋮ Open Access Journal

Received September 22, 2019, accepted October 5, 2019, date of publication October 25, 2019, date of current version November 5, 2019.

Digital Object Identifier 10.1109/ACCESS.2019.2947629

State Constraint Control for Uncertain Nonlinear Systems With Disturbance Compensation

ZHANGBAO XU[1,2], LAN LI[3], JIANYONG YAO[4], XIAOLEI HU[2], QINGYUN LIU[2], AND NENGGANG XIE[2]

[1]Engineering Research Center of Hydraulic Vibration and Control, Ministry of Education, Anhui University of Technology, Ma'anshan 234002, China
[2]School of Mechanical Engineering, Anhui University of Technology, Ma'anshan 234002, China
[3]China Academy of Launch Vehicle Technology, Beijing 100076, China
[4]School of Mechanical Engineering, Nanjing University of Science and Technology, Nanjing 210094, China

Corresponding author: Jianyong Yao (jerryyao.buaa@gmail.com)

This work was supported in part by the National Key R&D Programs of China under Grant 2017YFC0805100, in part by the National Natural Science Foundation of China under Grant 51675279, in part by the Anhui Science and Technology Project under Grant 1704a0902008, and in part by the Natural Science Foundation, Higher Education Institutions of Anhui Province, under Grant KJ2017A062.

ABSTRACT In this paper, a state constraint controller with disturbance compensation is proposed for uncertain nonlinear systems to improve the control performance without violating the full state constraints. A series of extended state observers are designed to estimate disturbances that include the unmodeled dynamics and the modeling errors. To guarantee non-violation of state constraints while compensating the disturbances, based on the backstepping technique, the state constraint controller with extended state observer is proposed by using the barrier Lyapunov function. Then, the stability of the closed-loop system is proved theoretically. Moreover, exponentially asymptotic tracking is achieved when the disturbances are not time-variant. Finally, the effectiveness of the proposed approach is verified by two examples.

INDEX TERMS Uncertain nonlinear systems, state constraint, extended state observer, disturbance compensation.

I. INTRODUCTION

Disturbances (include the unmodeled dynamics, the modeling errors) always exist in all practical control systems, which may lead to tracking accuracy degradation and even the instability of system. The controller design for nonlinear system has received a great deal of attention due to the requirements in practical applications and theoretical challenges [1]–[3]. In order to weaken the influence of disturbances, as a main choice, nonlinear robust control has been widely used to attenuate disturbances, such as adaptive robust control [2], sliding mode control [4], super-twisting control [5], continuous nonsingular terminal sliding mode control [6], adaptive control with RISE feedback [7]. Simulations and experiments show that these robust controllers guarantee prescribed output tracking performance. However, large feedback gain might be used to guarantee the high control precision in the abovementioned robust controllers, which may lead to high gain feedback and even system instability.

The associate editor coordinating the review of this manuscript and approving it for publication was Ding Zhai.

In order to reduce the conservatism of the controller and improve the control performance without high-gain feedback, disturbance compensation in nonlinear systems has been wildly studied [8]–[16]. Various disturbance observers, such as uncertainty and disturbance estimator [10], [15], nonlinear disturbance observer [11], extended state observer [9], [16], and finite-time disturbance observer [13], are designed to estimate the generalized disturbances/uncertainties. These studies show that these disturbance observers have good performance and the system can achieve high performance control through disturbance compensation without high gain feedback. Especially in [9] and [16], the active disturbance rejection control (ADRC) is proposed for large disturbances, an extended state observer is used in the design of ADRC to estimate disturbances and compensate them in real time. As the excellent performance and very little information about the plant dynamics are required, ADRC is used widely [17]–[21]. However, the abovementioned results do not take into account the effect of state constraints.

In fact, many practical systems are subject to constraint, such as physical stoppages and the temperature of chemical reactor. Recently, Barrier Lyapunov Functions (BLFs) [22]–[25] are widely used to deal with the control problem of nonlinear systems with full state constraints [26]–[28]. To solve the control problem of nonlinear systems with a special class of dynamic uncertainties and full state constraints, an adaptive neural dynamic surface controller is designed for strict-feedback nonlinear systems in [29]. Then, adaptive neural dynamic surface control is developed using radial basis function neural networks for a class of pure-feedback nonlinear systems [30]. An improved adaptive neural dynamic surface controller is designed for pure-feedback systems with full state constraints and disturbance in [31]. For non-strict feedback systems with full-state constraints and unmodeled dynamics, adaptive neural-based control is proposed in [32]. These controllers can guarantee good tracking performance. However, neural network is used in all the above controllers, the estimations are obtained based on the neural weight vector and the number of adjustable parameters will be enormous if the neural network nodes increase. Then, the online learning time becomes very large. Besides, disturbances have not been effectively dealt with. In some cases, disturbances may be the main obstacles to systems and will greatly reduce the performance and constrainability of states of the system.

As the problem of state constraint control with disturbance compensation for uncertain nonlinear systems with full state constraints and disturbances has not been effectively discussed. The problem is still open and unsolved. Based on the above works, in this paper, for a general class of nonlinear systems with full state constrains and disturbances, based the ADRC technique for disturbances, state constraint control with disturbance compensation is proposed. The main contributions of the proposed approach are that:

1) This paper frames a generalization of the results for a general class of nonlinear pure-feedback systems with the full state constraints and general disturbances; For the first time, ADRC is introduced into the field of full-state constrained control. The radically different operation principle of the full state constraint control and ADRC are synthesized to avoid the violation of full state constraints and handle disturbances, and the theoretical results of the two design methods are retained.

2) State constraint control with disturbance compensa- tion via BLF combined with ESO is designed. ESO is employed to estimate disturbances of all channels and avoiding high-gain feedback. The BLF guarantees that the full state constraints are not violated and all the closed-loop signals remain bounded. Moreover, the control perfor-mance can be guaranteed theoretically by the proposed controller while exponentially asymptotic tracking is achieved when the disturbances are not time-variant.

The paper is organized as follows: Section II presents problem formulation and preliminaries. In Section III, the ESO and state constraint control scheme are given. The effectiveness is demonstrated by application of the proposed approach in two examples in Section IV, and Section V gives conclusion.

II. PROBLEM FORMULATION AND PRELIMINARIES

Consider a class of uncertain nonlinear systems with disturbances:

$$\begin{cases} \dot{x}_i = \mu_i(\bar{x}_i)\, x_{i+1} + G_i(\bar{x}_i) + \Delta_i(\bar{x}_i, t), \ 1 \le i \le n-1 \\ \dot{x}_n = \mu_n(x)\, u + G_n(x) + \Delta_n(x, t) \\ y = x_1 \end{cases} \tag{1}$$

where $x = [x_1, x_2, \ldots, x_n]^{\mathrm{T}} \in R^n$ and $\bar{x}_i = [x_1, x_2, \ldots, x_i]^{\mathrm{T}} \in R^i$ are system states, all the states are constrained in the compact sets as $\Omega_{x_i} = \{x_i : |x_i| \le k_{c_i}, i = 1, \ldots, n\}$ with k_{c_i} being positive constants;$u \in R$ is control input; $y \in R$ is system output;$\mu_i(\cdot)$ are known and bounded nonlinear functions, which are smooth enough, i.e., there exist the constants $\bar{\mu}_i \ge \underline{\mu}_i > 0$ such that $\underline{\mu}_i \le |\mu_i(\cdot)| \le \bar{\mu}_i$; $G_i(\bar{x}_i) \in R$ and $G_n(\underline{x_n}) \in R$ are known smooth system state functions;$\Delta_i(\bar{x}_i, t) \in R$, $i = 1, \ldots, n$, are unknown smooth nonlinear disturbances. The following assumptions are made for ESO.

Remark 1: For the considered system (1), in order to design the controller expediently, we let the nonlinear functions μ_i be smooth and bounded. A very common case satisfied this limitation is that $\mu_1(\bar{x}_1) = \mu_2(\bar{x}_2) = \cdots = \mu_n(x) = 1$.

Assumption 1: Δ_i and the time derivative $\dot{\Delta}_i$ are bounded, i.e., there exist the constants $\bar{\Delta}_i > 0$, $\bar{\Delta}_{id} > 0$ satisfying

$$|\Delta_i| \le \bar{\Delta}_i, \quad \left|\dot{\Delta}_i\right| \le \bar{\Delta}_{id}, \ i = 1, ..., n. \tag{2}$$

Remark 2: For ESO-based design, **Assumption 1** is a fundamental precondition and has been widely used in [6], [17], [18], [33], and [34], and these studies have proved that this assumption is appropriate to physical applications.

Assumption 2 [35]: It is assumed that desired trajectory $x_{1d}(t)$ and its i_{th} order derivatives $x_{1d}^{(i)}(t)$, $i = 1, \ldots, n$ satisfy $x_{1d}(t) \le \rho_0 \le k_{c_1} - L_1$ and $\left|x_{1d}^{(i)}(t)\right| \le \rho_i$ where $\rho_0, \rho_1, \ldots, \rho_n$ are positive constants, L_1 is positive parameter used later.

For the desired trajectory $x_{1\,d}(t)$, our objective is to design control input u such that the output x_1 tracks $x_{1\,d}(t)$ as closely as possible in spite of disturbances while ensuring that the system constraints are not violated. To prevent the system states from violating the constraints, the BLF is employed.

III. CONTROLLER DESIGN AND STABILITY ANALYSIS

A. EXTENDED STATE OBSERVER DESIGN

For system (1), ESOs are employed to estimate matched disturbance and unmatched disturbances simultaneously. Firstly, we extend $x_{ei}(\bar{x}_i, t) = \Delta_i$, $i = 1, \ldots, n$, let $h_i(\bar{x}_i, t)$ be the time derivatives of $x_{ei}(\bar{x}_i, t)$. Then, rewrite (1), we have

$$\begin{cases} \dot{x}_i = \mu_i(\bar{x}_i)\, x_{i+1} + G_i(\bar{x}_i) + x_{ei}(\bar{x}_i, t) \\ \dot{x}_{ei} = h_i(\bar{x}_i, t), \ i = 1, \ldots, n-1 \end{cases}$$
$$\begin{cases} \dot{x}_n = \mu_n(x)\, u + G_n(x) + x_{en}(x, t) \\ \dot{x}_{en} = h_n(x, t) \end{cases} \tag{3}$$

For (3), the structures of ESOs are designed to be

$$\begin{cases} \dot{\hat{x}}_i = \mu_i(\bar{x}_i)\,x_{i+1} + G_i(\bar{x}_i) + \hat{x}_{ei}(\bar{x}_i, t) + l_1\omega_i(x_i - \hat{x}_i) \\ \dot{\hat{x}}_{ei} = l_2\omega_i^2(x_i - \hat{x}_i),\ i = 1, \ldots, n-1 \end{cases}$$
$$\begin{cases} \dot{\hat{x}}_n = \mu_n(x)\,u + G_n(x) + \hat{x}_{en}(x, t) + l_1\omega_n(x_n - \hat{x}_n) \\ \dot{\hat{x}}_{en} = l_2\omega_n^2(x_n - \hat{x}_n) \end{cases} \tag{4}$$

where $\hat{x}_i$ denote the estimation of x_i, $\hat{x}_{ei}$ denote the estimation of x_{ei}. $\omega_i > 0$, $i = 1, \ldots, n$ are parameters of ESO to be given later, l_1 and l_2 are coefficients of the Hurwitz polynomial $s^2 + l_1 s + l_2$.

Remark 3: Different from [36] and [37], it is interesting that the states of the system are estimated simultaneously when the system disturbances are estimated. This is determined by the structure of the extended state observer, because the estimation of system disturbances is driven by the state estimation error, which requires both the known system state and the estimated state.

Noting (3) and (4), the dynamic of estimation errors can be given as follow

$$\begin{cases} \dot{\tilde{x}}_i = \tilde{x}_{ei} - l_1\omega_i\tilde{x}_i \\ \dot{\tilde{x}}_{ei} = h_i(\bar{x}_i, t) - l_2\omega_i^2\tilde{x}_i, \end{cases} \quad i = 1, \ldots, n \tag{5}$$

where $\tilde{\bullet} = \bullet - \hat{\bullet}$.

Define $\varepsilon_i = [\varepsilon_{i1}, \varepsilon_{i2}]^T = [\tilde{x}_i, \tilde{x}_{ei}/\omega_i]^T$, $i = 1, \ldots, n$, we have

$$\dot{\varepsilon}_i = \omega_i A\varepsilon_i + B\frac{h_i(\bar{x}_i, t)}{\omega_i} \tag{6}$$

where $A = \begin{bmatrix} -l_1 & 1 \\ -l_2 & 0 \end{bmatrix}$, $B = [0, 1]^T$.

As the matrix A is Hurwitz, we can select a positive definite matrix P satisfying

$$A^T P + PA = -2I \tag{7}$$

where the matrix I is an identity matrix.

B. CONTROLLER DESIGN

Define $z_1 = x_1 - x_{1d}$, $z_i = x_i - \alpha_{i-1}$, $i = 2, \ldots, n$, α_{i-1} is virtual controller. In order to keep the constraints of $z_1, z_2, \ldots, z_n$ and achieve the constraints of $x_1, x_2, \ldots, x_n$, the full state constraint controller design process is presented as follow.

Step 1: Define a positive definite BLF

$$V_1 = \frac{1}{2}b_1\log\frac{L_1^2}{L_1^2 - z_1^2} \tag{8}$$

where b_1 and $L_1 = k_{c_1} - \rho_0$ are positive parameters, $\log(\chi)$ is the natural logarithm of χ.

Noting (1), the time derivative of V_1 is

$$\begin{aligned} \dot{V}_1 &= \frac{b_1 z_1(\mu_1(\bar{x}_1)\,x_2 + G_1(\bar{x}_1) + \Delta_1(\bar{x}_1, t) - \dot{x}_{1d})}{L_1^2 - z_1^2} \\ &= \frac{b_1 z_1(\mu_1(\bar{x}_1)(z_2 + \alpha_1) + G_1(\bar{x}_1) + \Delta_1(\bar{x}_1, t) - \dot{x}_{1d})}{L_1^2 - z_1^2} \end{aligned} \tag{9}$$

Based on the disturbance estimation by ESOs in (4), the virtual α_1 is designed to be

$$\alpha_1 = \left(-G_1(\bar{x}_1) - \hat{x}_{e1} + \dot{x}_{1d} - k_1 z_1 - \frac{b_1\omega_1^2 z_1}{2(L_1^2 - z_1^2)}\right)/\mu_1(\bar{x}_1) \tag{10}$$

where $k_1 > 0$ is controller parameter to be determined later.

Then, noting (9) and making use of the Young's inequality, the dynamic $\dot{V}_1$ becomes

$$\begin{aligned} \dot{V}_1 &= \frac{-k_1 b_1 z_1^2}{L_1^2 - z_1^2} + \frac{b_1\mu_1(\bar{x}_1)\,z_1 z_2}{L_1^2 - z_1^2} + \frac{b_1 z_1\omega_1\varepsilon_{12}}{L_1^2 - z_1^2} - \frac{b_1^2\omega_1^2 z_1^2}{2(L_1^2 - z_1^2)^2} \\ &\le \frac{-k_1 b_1 z_1^2}{L_1^2 - z_1^2} + \frac{b_1\mu_1(\bar{x}_1)\,z_1 z_2}{L_1^2 - z_1^2} + \frac{\varepsilon_{12}^2}{2} \end{aligned} \tag{11}$$

Step i ($2 \le i \le n-1$): Define positive definite BLF

$$V_i = \frac{1}{2}b_i\log\frac{L_i^2}{L_i^2 - z_i^2} + V_{i-1}, \quad i = 2, \ldots, n-1 \tag{12}$$

where b_i and L_i are positive parameters.

Noting (1), the time derivative of V_i is

$$\begin{aligned} \dot{V}_i &= \frac{b_i z_i\dot{z}_i}{L_i^2 - z_i^2} + \dot{V}_{i-1} \\ &= \frac{b_i z_i(\mu_i(\bar{x}_i)(z_{i+1} + \alpha_i) + G_i(\bar{x}_i) + \Delta_i(\bar{x}_i, t) - \dot{\alpha}_{i-1})}{L_i^2 - z_i^2} + \dot{V}_{i-1} \end{aligned} \tag{13}$$

Similar to (10), the virtual α_i is designed to be

$$\alpha_i = \begin{pmatrix} -G_i(\bar{x}_i) - \hat{x}_{ei} + \dot{\alpha}_{(i-1)c} - k_i z_i - \frac{b_i\omega_i^2 z_i}{2(L_i^2 - z_i^2)} \\ -\frac{\mu_{i-1}b_{i-1}z_{i-1}(L_i^2 - z_i^2)}{b_i(L_{i-1}^2 - z_{i-1}^2)} - \frac{b_i\sum_{k=1}^{i-1}\left(\omega_k\frac{\partial\alpha_{i-1}}{\partial x_k}\right)^2 z_i}{2(L_i^2 - z_i^2)} \end{pmatrix}/\mu_i(\bar{x}_i) \tag{14}$$

where $k_i > 0$ is controller parameter to be determined later. $\dot{\alpha}_{i-1} = \dot{\alpha}_{(i-1)c} + \dot{\alpha}_{(i-1)u}$, $\dot{\alpha}_{(i-1)c}$ is the calculable part, $\dot{\alpha}_{(i-1)u}$ is the incalculable part.

$$\begin{aligned} \dot{\alpha}_{(i-1)c} &= \frac{\partial\alpha_{i-1}}{\partial t} \\ &\quad + \sum_{k=1}^{i-1}\frac{\partial\alpha_{i-1}}{\partial x_k}(\mu_k(\bar{x}_k)\,x_{k+1} + G_k(\bar{x}_k) + \hat{x}_{ek}(\bar{x}_k, t)) \\ &\quad + \sum_{h=1}^{i-2}\frac{\partial\alpha_{i-1}}{\partial\hat{x}_h}(\mu_h(\bar{x}_h)\,x_{h+1} \\ &\quad + G_h(\bar{x}_h) + \hat{x}_{eh}(\bar{x}_h, t) + l_1\omega_h(x_h - \hat{x}_h)) \\ &\quad + \sum_{k=1}^{i-1}\frac{\partial\alpha_{i-1}}{\partial\hat{x}_{ek}}\left(l_2\omega_k^2(x_k - \hat{x}_k)\right), \\ \dot{\alpha}_{(i-1)u} &= \sum_{k=1}^{i-1}\frac{\partial\alpha_{i-1}}{\partial x_k}(\tilde{x}_{ek}(\bar{x}_k, t)) \end{aligned} \tag{15}$$

Then, we have

$$\dot{V}_i = \dot{V}_{i-1} - \frac{b_i k_i z_i^2}{L_i^2 - z_i^2} + \frac{b_i \mu_i(\bar{x}_i) z_i z_{i+1}}{L_i^2 - z_i^2} + \frac{b_i z_i \left(\omega_i \varepsilon_{i2} - \sum_{k=1}^{i-1} \frac{\partial \alpha_{i-1}}{\partial x_k} (\tilde{x}_{ek}(\bar{x}_k, t))\right)}{L_i^2 - z_i^2} - \frac{\mu_{i-1} b_{i-1} z_i z_{i-1}}{L_{i-1}^2 - z_{i-1}^2} - \frac{b_i^2 \omega_i^2 z_i^2}{2(L_i^2 - z_i^2)^2} - \frac{b_i^2 z_i^2 \sum_{k=1}^{i-1} \left(\omega_k \frac{\partial \alpha_{i-1}}{\partial x_k}\right)^2}{2(L_i^2 - z_i^2)^2} \quad (16)$$

Applying the Young's inequality, we obtain

$$\frac{b_i z_i \omega_i \varepsilon_{i2}}{L_i^2 - z_i^2} \le \frac{b_i^2 \omega_i^2 z_i^2}{2(L_i^2 - z_i^2)^2} + \frac{\varepsilon_{i2}^2}{2},$$

$$\frac{b_i z_i \sum_{k=1}^{i-1} \frac{\partial \alpha_{i-1}}{\partial x_k} (\tilde{x}_{ek}(\bar{x}_k, t))}{L_i^2 - z_i^2} \le \frac{\sum_{k=1}^{i-1} \varepsilon_{k2}^2}{2} + \frac{b_i^2 z_i^2 \sum_{k=1}^{i-1} \left(\omega_k \frac{\partial \alpha_{i-1}}{\partial x_k}\right)^2}{2(L_i^2 - z_i^2)^2}.$$

The above inequalities are employed, (16) becomes

$$\dot{V}_i \le \dot{V}_{i-1} - \frac{b_i k_i z_i^2}{L_i^2 - z_i^2} + \frac{b_i \mu_i(\bar{x}_i) z_i z_{i+1}}{L_i^2 - z_i^2} + \frac{\sum_{k=1}^{i} \varepsilon_{k2}^2}{2} - \frac{\mu_{i-1} b_{i-1} z_i z_{i-1}}{L_{i-1}^2 - z_{i-1}^2} \quad (17)$$

Then, we have

$$\dot{V}_i \le \frac{b_i \mu_i(\bar{x}_i) z_{i+1} z_i}{L_i^2 - z_i^2} - \sum_{k=1}^{i} \frac{k_k b_k z_k^2}{L_k^2 - z_k^2} + \sum_{j=1}^{i} \sum_{k=1}^{j} \frac{\varepsilon_{k2}^2}{2} \quad (18)$$

Step n: Define a positive definite BLF

$$V_n = \frac{1}{2} b_n \log \frac{L_n^2}{L_n^2 - z_n^2} + V_{n-1} \quad (19)$$

where $b_n > 0$ and $L_n > 0$ are parameters.

Noting (1), the time derivative of V_n is

$$\dot{V}_n = \frac{b_n z_n (\dot{x}_n - \dot{\alpha}_{n-1})}{L_n^2 - z_n^2} + \dot{V}_{n-1} = \frac{b_n z_n (\mu_n(x) u + G_n(x) + \Delta_n(x,t) - \dot{\alpha}_{n-1})}{L_n^2 - z_n^2} + \dot{V}_{n-1} \quad (20)$$

The input u is designed as follow

$$u = \frac{1}{\mu_n(x)} \left(\begin{array}{l} -G_n(x) - \hat{x}_{en} + \dot{\alpha}_{(n-1)c} - k_n z_n - \frac{b_n \omega_n^2 z_n}{2(L_n^2 - z_n^2)} \\ -\frac{\mu_{n-1} b_{n-1} z_{n-1} (L_n^2 - z_n^2)}{b_n (L_{n-1}^2 - z_{n-1}^2)} - \frac{b_n \sum_{k=1}^{n-1} \left(\omega_k \frac{\partial \alpha_{n-1}}{\partial x_k}\right)^2 z_n}{2(L_n^2 - z_n^2)} \end{array} \right) \quad (21)$$

where $k_n > 0$ is controller parameter to be designed later and $\dot{\alpha}_{n-1} = \dot{\alpha}_{(n-1)c} + \dot{\alpha}_{(n-1)u}$, $\dot{\alpha}_{(n-1)c}$ is the calculable part, $\dot{\alpha}_{(n-1)u}$ is the incalculable part.

$$\begin{aligned} \dot{\alpha}_{(n-1)c} &= \frac{\partial \alpha_{n-1}}{\partial t} + \sum_{k=1}^{n-1} \frac{\partial \alpha_{n-1}}{\partial x_k} (\mu_k(\bar{x}_k) x_{k+1} + G_k(\bar{x}_k) + \hat{x}_{ek}(\bar{x}_k, t)) \\ &\quad + \sum_{h=1}^{n-2} \frac{\partial \alpha_{n-1}}{\partial \hat{x}_h} (\mu_h(\bar{x}_h) x_{h+1} + G_h(\bar{x}_h) + \hat{x}_{eh}(\bar{x}_h, t) + l_1 \omega_h (x_h - \hat{x}_h)) \\ &\quad + \sum_{k=1}^{n-1} \frac{\partial \alpha_{n-1}}{\partial \hat{x}_{ek}} \left(l_2 \omega_k^2 (x_k - \hat{x}_k)\right), \\ \dot{\alpha}_{(n-1)u} &= \sum_{k=1}^{n-1} \frac{\partial \alpha_{n-1}}{\partial x_k} (\tilde{x}_{ek}(\bar{x}_k, t)) \end{aligned} \quad (22)$$

Put (21) into (20), we have

$$\begin{aligned} \dot{V}_n &= \dot{V}_{n-1} + \frac{b_n z_n (\Delta_n(x,t) - \hat{x}_{en} - \dot{\alpha}_{(n-1)u} - k_n z_n)}{L_n^2 - z_n^2} - \frac{\mu_{n-1} b_{n-1} z_{n-1} z_n}{L_{n-1}^2 - z_{n-1}^2} - \frac{b_n^2 \omega_n^2 z_n^2}{2(L_n^2 - z_n^2)^2} \\ &\quad \times \frac{b_n^2 \sum_{k=1}^{n-1} \left(\omega_{n-1} \frac{\partial \alpha_{n-1}}{\partial x_k}\right)^2 z_n^2}{2(L_n^2 - z_n^2)^2} \\ &\le -\sum_{j=1}^{n} \frac{k_j b_j z_j^2}{L_j^2 - z_j^2} + \sum_{j=1}^{n} \sum_{k=1}^{j} \frac{\varepsilon_{k2}^2}{2} \end{aligned} \quad (23)$$

Then, we have the following theorem.

Theorem 1: For the systems (1) with **Assumptions 1**, the virtual controller α_i, $i = 1, \ldots, n-1$ in (10), (14) and the actual controller u in (21), if the following conditions hold:

(1) choose appropriate design parameters k_i, b_i, ω_i and L_i to satisfy

$$k_{c_{i+1}} \ge |\alpha_i|_{\max} + L_{i+1}$$

(2) the initial conditions $z_i(0)$ belong to the set

$$\Omega_{z_i} = \{|z_i| \le L_i, i = 1, \ldots, n\}$$

The proposed state constraint controller ensures that: the $z_i(t)$ remain in the compact set Ω_{z_i}, all signals are bounded in the closed-loop system, and the full state constraints are not violated. Moreover, when the disturbances are not time-variant, i.e., $h_i(\bar{x}_i, t) = 0$, exponentially asymptotic tracking is achieved.

Proof: Defining a positive definite Lyapunov function

$$V_a = V_n + \sum_{i=1}^{n} \frac{1}{2} \varepsilon_i^T P \varepsilon_i \quad (24)$$

Noting (5), the time derivative of V_a is

$$\dot{V}_a = \dot{V}_n+\sum_{i=1}^{n}\left(\frac{1}{2}\dot{\varepsilon}_i^T P\varepsilon_i+\frac{1}{2}\varepsilon_i^T P\dot{\varepsilon}_i\right) = \dot{V}_n+\sum_{i=1}^{n}\left(\frac{1}{2}\omega_i\varepsilon_i^T A^T P\varepsilon_i+\frac{1}{2}\omega_i\varepsilon_i^T PA\varepsilon_i+\varepsilon_i^T PB\frac{h_i(\bar{x}_i,t)}{w_i}\right) \tag{25}$$

As $A^TP+PA=-2I$ and $\log\frac{L_j^2}{L_j^2-z_j^2}\leq\frac{z_j^2}{L_j^2-z_j^2}$ in the interval $z_j<L_j$ [38]. We have

$$\begin{aligned}\dot{V}_a &\leq \dot{V}_n-\sum_{i=1}^{n}\omega_i\|\varepsilon_i\|^2+\sum_{i=1}^{n}\varepsilon_i^T PB\frac{h_i(\bar{x}_i,t)}{\omega_i}\\ &\leq -\sum_{j=1}^{n}\frac{k_jb_jz_j^2}{L_j^2-z_j^2}-\sum_{i=1}^{n}\omega_i\|\varepsilon_i\|^2+\sum_{j=1}^{n}\sum_{k=1}^{j}\frac{\varepsilon_{k2}^2}{2}\\ &\quad+\frac{1}{2}\sum_{i=1}^{n}\|\varepsilon_i\|^2+\sum_{i=1}^{n}\frac{\|\varepsilon_i\|^2}{2}+\sum_{i=1}^{n}\frac{\|PB\|^2|h_i(\bar{x}_i,t)|_{\max}^2}{2\omega_i^2}\\ &\leq -\sum_{j=1}^{n}k_jb_j\log\frac{L_j^2}{L_j^2-z_j^2}-\sum_{i=1}^{n}\frac{2\omega_i-n-2}{2\lambda_{\max}(P)}\varepsilon_i^TP\varepsilon_i+\sigma\\ &\leq -\lambda V_a+\sigma\end{aligned} \tag{26}$$

where

$$\lambda=\left\{2k_1,\ldots,2k_n,\frac{2\omega_1-n-2}{2\lambda_{\max}(P)},\ldots,\frac{2\omega_n-n-2}{2\lambda_{\max}(P)}\right\}_{\min},$$
$$\sigma=\sum_{i=1}^{n}\frac{\|PB\|^2|h_i(\bar{x}_i,t)|_{\max}^2}{2\omega_i^2}.$$

From (26), we can obtain

$$V_a(t)\leq\exp(-\lambda t)V_a(0)+\frac{\sigma}{\lambda}\left[1-\exp(-\lambda t)\right] \tag{27}$$

From (27), we have $\frac{1}{2}b_i\log\frac{L_i^2}{L_i^2-z_i^2}\leq\exp(-\lambda t)V_a(0)+\frac{\sigma}{\lambda}\left[1-\exp(-\lambda t)\right], i=1,\ldots,n$, we can obtain $|z_i|\leq L_i\sqrt{1-e^{-\frac{2}{b_i}\left[V_a(0)+\frac{\sigma}{\lambda}\right]}}$. From $x_1=z_1+x_{1d}(t)$, we have $|x_1|\leq L_1+|x_{1d}(t)|_{\max}\leq k_{c_1}$, x_1 is bounded. It is obvious that α_1 in (10) is a function of x_1, z_1, $\dot{x}_{1d}$ and x_{e1}. Since the boundedness of x_1, z_1, $\dot{x}_{1d}$ and x_{e1}, α_1 is bounded. As $|z_2|\leq L_2$, $|x_2|\leq|\alpha_1|_{\max}+|z_2|\leq k_{c_2}$, then x_2 is bounded. Similarly, we have $|x_{i+1}|\leq k_{c_{i+1}}$, $i=2,\ldots,n$-1. From the definitions of u and α_i, $i=1,\ldots,n$-1, it is obvious that the controller u and α_i are bounded. From the above analysis, all the signals are bounded, and the full state constraints are not violated. Moreover, when the disturbances are not time-variant, i.e., $h_i(\bar{x}_i,t)=0$, from (26), we have $\dot{V}_a\leq-\lambda V_a$, and exponentially asymptotic tracking is achieved.

IV. SIMULATION RESULTS

In order to testify the effectiveness of the proposed approach, two simulation examples are given.

Example 1: Similar to [39], the second-order nonlinear system is given as follow:

$$\begin{aligned}\dot{x}_1 &= 0.1x_1^2+x_2+d_1(x,t)\\ \dot{x}_2 &= \left(1+x_1^2\right)u+0.1x_1x_2-0.2x_1+d_2(x,t)\end{aligned} \tag{28}$$

where the states are constrained in $|x_1|\leq 1, |x_2|\leq 40$, the desired trajectory $x_{1d}(t)=0.5\sin(t)$, $d_1(x,t)=30\sin(\pi t)$, $d_2(x,t)=50\sin(\pi t)$. Let $x_{ei}(x,t)=d_i(x,t)$, $i=1,2$. Two ESOs are designed as follow

$$\begin{cases}\dot{\hat{x}}_1=0.1x_1^2+x_2+\hat{x}_{e1}+2\omega_1(x_1-\hat{x}_1)\\ \dot{\hat{x}}_{e1}=\omega_2^2(x_1-\hat{x}_1)\end{cases}$$
$$\begin{cases}\dot{\hat{x}}_2=\left(1+x_1^2\right)u+0.1x_1x_2-0.2x_2+\hat{x}_{e2}+2\omega_2(x_2-\hat{x}_2)\\ \dot{\hat{x}}_{e2}=\omega_2^2(x_2-\hat{x}_2)\end{cases} \tag{29}$$

Define $z_1=x_1$-x_{1d}, $z_2=x_2$-α_1, the final control input u and virtual control law are designed as

$$\begin{aligned}u &= \frac{1}{1+x_1^2}\begin{bmatrix}-0.1x_1x_2+0.2x_2-\hat{x}_{e2}+\dot{\alpha}_{1c}-\frac{b_1}{b_2}\frac{L_2^2-z_2^2}{L_1^2-z_1^2}z_1\\ -k_2z_2-\frac{b_2\omega_2^2z_2}{2(L_2^2-z_2^2)}-\frac{b_2\left(\frac{\partial\alpha_1}{\partial x_1}\right)^2\omega_1^2z_2}{2(L_2^2-z_2^2)}\end{bmatrix}\\ \dot{\alpha}_{1c} &= \frac{\partial\alpha_1}{\partial t}+\frac{\partial\alpha_1}{\partial x_1}\left(0.1x_1^2+x_2+\hat{x}_{e1}\right)+\frac{\partial\alpha_2}{\partial\hat{x}_{e1}}\dot{\hat{x}}_{e1}\\ \alpha_1 &= -0.1x_1^2-\hat{x}_{e1}+\dot{x}_{1d}-k_1z_1-\frac{b_1\omega_1^2z_1}{2\left(L_1^2-z_1^2\right)}\end{aligned} \tag{30}$$

In the simulation, the initial states are $x_1(0)=0.4$, $x_2(0)=20$. The following four controllers are applied to test the validity of the proposed controller:

SCCDC: The state constraint controller with disturbance compensation proposed in (30). The control parameters are selected as $k_1=40, k_2=50, b_1=3, b_2=0.1, L_1=1, L_2=50, \omega_1=200, \omega_2=300$.

FNRCDC: The feedback nonlinear robust controller with disturbance compensation, the controller is given as $u=\frac{1}{1+x_1^2}\left[-0.1x_1x_2+0.2x_2-\hat{x}_{e2}+\dot{\alpha}_{1c}-k_2z_2\right]$, where $\dot{\alpha}_{1c}=\frac{\partial\alpha_1}{\partial t}+\frac{\partial\alpha_1}{\partial x_1}\dot{\hat{x}}_1+\frac{\partial\alpha_2}{\partial\hat{x}_{e1}}\dot{\hat{x}}_{e1}, \alpha_1=-0.1x_1^2-\hat{x}_{e1}+\dot{x}_{1d}-k_1z_1$. The controller gains are given as $k_1=200$, $k_2=300$, $\omega_1=200, \omega_2=300$.

FLC: The feedback linearization controller without disturbance compensation. The controller gains are given as $k_1=200, k_2=300$.

RFC: The robust feedback controller only with the linear robust feedback term and without disturbance compensation and model compensation term. The feedback gains are selected same as corresponding feedback gains of the FNRCDC controller.

Remark 4: We can verify the validity of model compensation term by compare RFC with FLC. The validity of disturbance compensation term can be verified by the comparison between FLC and FNRCDC. The comparison between FNRCDC and SCCDC can verify the validity of state constraint term. Hence, by comparison of the

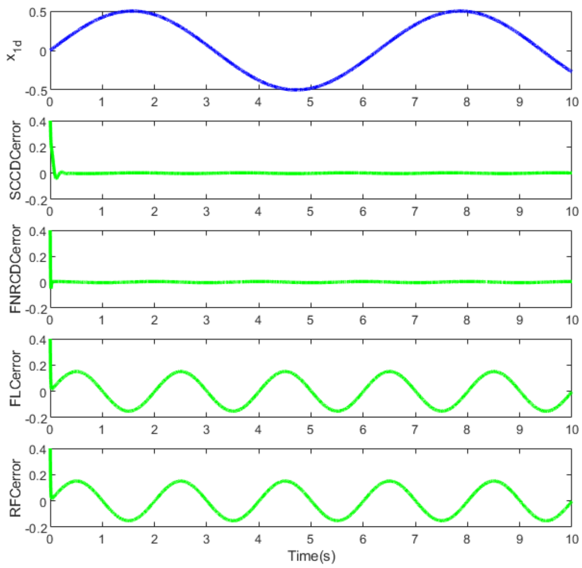

FIGURE 1. The desired trajectory x_{1d} and tracking error of controllers.

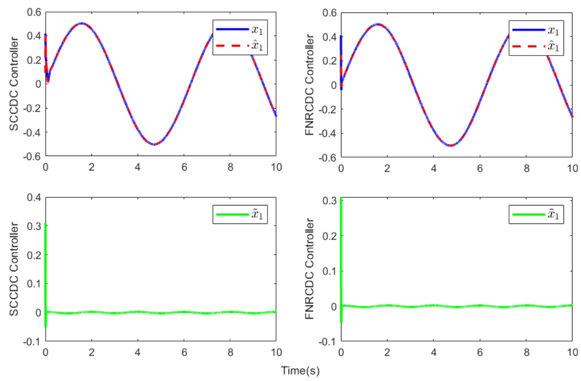

FIGURE 2. x_1, estimation of x_1 and estimation error.

four controllers, the validity of the proposed controller can be tested.

From Fig.1, it is clearly that SCCDC (the tracking error is about 2.5×10^{-3}) and FNRCDC (the tracking error is about 4.5×10^{-3}) achieve better tracking performance because of the accurate disturbance compensation. This verifies the effectiveness of disturbance compensation in SCCDC and FNRCDC. Tracking errors of RFC and FLC are much larger due to only some robustness of them against the modeling uncertainties. Due to the large disturbances of the system, the model compensation in FLC is almost useless, and the tracking errors of RFC and FLC are almost the same. The SCCDC has better tracking accuracy than FNRCDC, FLC and RFC, which demonstrates the advantage of the state constraint design and disturbance compensation procedure. In a word, the proposed SCCDC achieved best tracking performance with the help of the state constraint design and disturbance compensation. Fig.2 and Fig.3 present the state estimations and estimation errors of x_1 and x_2 in SCCDC and FNRCDC, respectively. As seen, the system steady-state

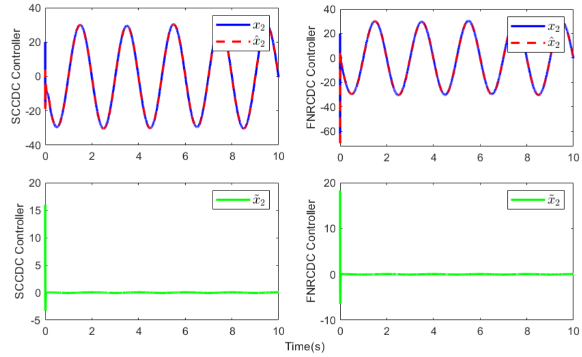

FIGURE 3. x_2, estimation of x_2 and estimation error.

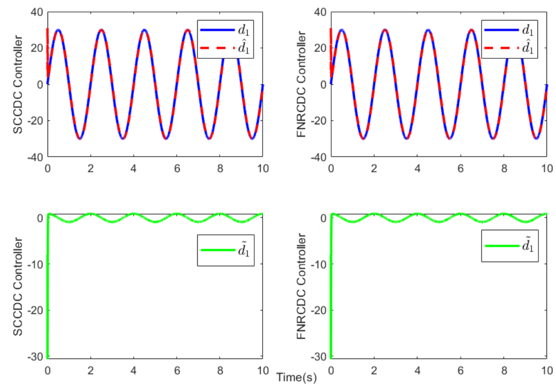

FIGURE 4. d_1, $\hat{d}_1$ and estimation error.

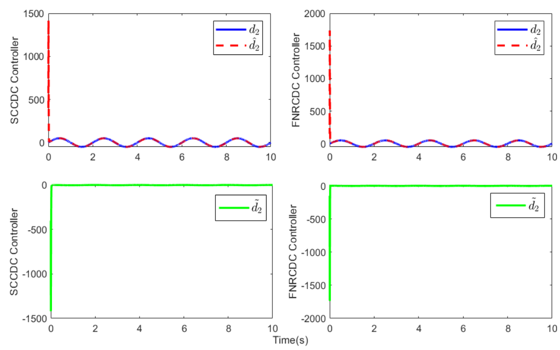

FIGURE 5. d_2, $\hat{d}_2$ and estimation error.

estimations are accurate even with big transient estimation errors caused by the unmatched system initial states. The disturbance estimation performance of the ESOs in SCCDC and FNRCDC is shown in Fig.4 and Fig.5, which verified the good performance of ESOs. The z_1, z_2 are illustrated in Fig.6. From this figure, it is obvious that the bounds for z_1, z_2 are not overstepped. The x_1, x_2 of SCCDC and FNRCDC are illustrated in Fig.7, the state constraints in SCCDC are not overstepped, while the state constraints in FNRCDC are overstepped, which illustrate the effectiveness of the state-constrained control strategy.

Example 2: simulation results of a dc motor-driven robot manipulator are obtained. The robot manipulator is considered to be a simple one-link manipulator. Similar to [6],

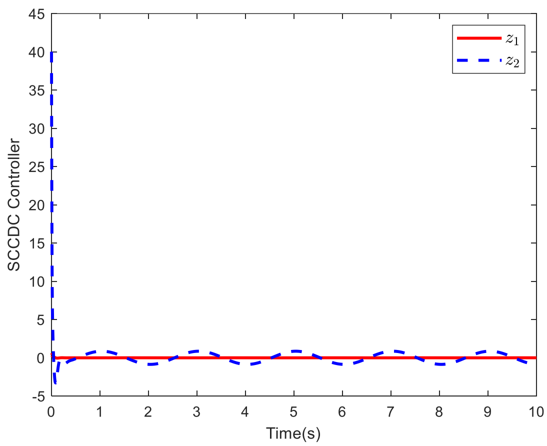

FIGURE 6. The graph of z_1 and z_2 of SCCDC Controller.

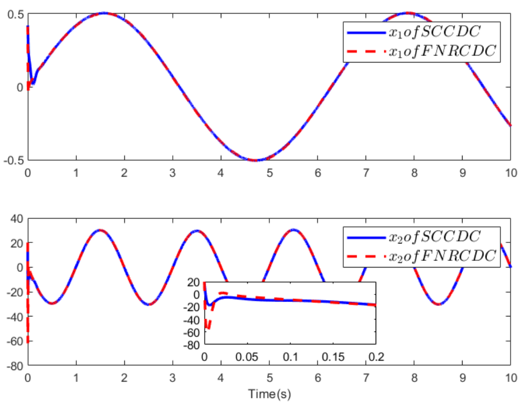

FIGURE 7. x_1 and x_2 of SCCDC Controller and FNRCDC Controller.

the dynamic equation of the inertial load is

$$m\ddot{\theta} = K_i i - b\dot{\theta} - f_d(x,t) \tag{31}$$

where m and θ represent the inertia load and the angular displacement, respectively; K_i denotes the torque constant relative to the unit of current; i and b denote the system current and the viscous friction coefficient, respectively; $f_d(x,t)$ is the unmodeled dynamic.

The current dynamic is modeled as follow

$$L\frac{di}{dt} = K_u u - Ri - K_R\dot{\theta} \tag{32}$$

where L and K_u denote the armature inductance of the motor and the electrical gain, respectively; u is the control input, R and K_R represent the armature resistance of the motor and the electromotive force coefficient, respectively.

Remark 5: Potential risks are always accompanied by the motion systems (like robot manipulator) driven by dc motor due to its fast response, especially in a large number of testing applications that involve reciprocity between unit under test (UUT) and environment. If the state constraints are ignored, the process safety may be in danger during testing process, the UUT may be damaged by excessive velocity and/or acceleration. In fact, when the initial state of the system does not match, it is possible to generate overlarge velocity and/or acceleration.

Define $x = [x_1, x_2, x_3]^{\mathrm{T}} = [\theta, \dot{\theta}, i]^{\mathrm{T}}$, rewrite the dynamic system model in a state-space form as follow

$$\begin{aligned} \dot{x}_1 &= x_2 \\ \dot{x}_2 &= \frac{K_i}{m}x_3 - \frac{b}{m}x_2 + d_1(x,t) \\ \dot{x}_3 &= \frac{K_u}{L}u - \frac{R}{L}x_3 - \frac{K_R}{L}x_2 + d_2(x,t) \end{aligned} \tag{33}$$

where $d_1(x,t) = \text{-}f_d(x,t)/m$ and $d_2(x,t) = 0$. The constraints of x_1, x_2, and x_3 are preset as $|x_1| \le 1$, $|x_2| \le 10$, $|x_3| \le 10$.

On the basis of the design process in Sect. 3.1, two ESOs are constructed to estimate the unmatched disturbance and matched disturbance, respectively. In order to weaken the noise effect, velocity signal is replaced by displacement signal to construct the first ESO, which is based on the former two equations. Let $x_{ei}(x,t) = d_i(x,t)$, $i = 1, 2$. Two ESOs are designed as follow

$$\begin{aligned} &\begin{cases} \dot{\hat{x}}_1 = \hat{x}_2 + 3\omega_1(x_1 - \hat{x}_1) \\ \dot{\hat{x}}_2 = \frac{K_i}{m}x_3 - \frac{b}{m}x_2 + \hat{x}_{e1} + 3\omega_1^2(x_1 - \hat{x}_1) \\ \dot{\hat{x}}_{e1} = \omega_1^3(x_1 - \hat{x}_1) \end{cases} \\ &\begin{cases} \dot{\hat{x}}_3 = \frac{K_u}{L}u - \frac{R}{L}x_3 - \frac{K_R}{L}x_2 + \hat{x}_{e2} + 2\omega_2(x_3 - \hat{x}_3) \\ \dot{\hat{x}}_{e2} = \omega_2^2(x_3 - \hat{x}_3) \end{cases} \end{aligned} \tag{34}$$

Then, we have the dynamic function of the observer estimation errors

$$\dot{\xi} = \omega_1 A_1 \xi + B_1\frac{h_2(x,t)}{\omega_1}, \; \dot{\mu} = \omega_2 A_2 \mu + B_2\frac{h_3(x,t)}{\omega_2} \tag{35}$$

where $\xi = [\tilde{x}_1, \tilde{x}_2, \tilde{x}_{e1}/\omega_1]^T$, $\mu = [\tilde{x}_3, \tilde{x}_{e2}/\omega_2]^T$, $B_1 = [0,0,1]^{\mathrm{T}}$, $B_2 = [0,0,1]^{\mathrm{T}}$. Since A_1 and A_2 are Hurwitz, we can choose two positive definite matrixes P_1, P_2 satisfying $A_1^T P_1 + P_1 A_1 = -I$, $A_2^T P_2 + P_2 A_2 = -I$, respecti-vely.

Define $z_1 = x_1\text{-}x_{1d}$, $z_2 = x_2\text{-}\alpha_1$, $z_3 = x_3\text{-}\alpha_2$, the final control input controller and virtual control law are designed as

$$\begin{aligned} u &= \frac{L}{K_u}\left[\begin{array}{l} \frac{R}{L}x_3 + \frac{K_R}{L}x_2 - \hat{x}_{e2} + \dot{\alpha}_{2c} - \frac{b_2 K_R}{b_3 m}\frac{L_3^2 - z_3^2}{L_2^2 - z_2^2}z_2 \\ -k_3 z_3 - \frac{b_3\omega_2^2 z_3}{2(L_3^2 - z_3^2)} - \frac{b_3\left(\frac{\partial\alpha_2}{\partial x_2}\right)^2\omega_2^4 z_3}{2(L_3^2 - z_3^2)} \end{array}\right] \\ \dot{\alpha}_{2c} &= \frac{\partial\alpha_2}{\partial t} + \frac{\partial\alpha_2}{\partial x_1}x_2 + \frac{\partial\alpha_2}{\partial x_2}\dot{\hat{x}}_2 + \frac{\partial\alpha_2}{\partial\hat{x}_{e1}}\dot{\hat{x}}_{e1} \\ \alpha_2 &= \frac{m}{K_i}\left(\frac{b}{m}x_2 + \dot{\alpha}_1 - \hat{x}_{e1} - k_2 z_2 \right. \\ &\qquad \left. - \frac{b_1}{b_2}z_1\frac{L_2^2 - z_2^2}{L_1^2 - z_1^2} - \frac{b_2\omega_1^4 z_2}{2(L_2^2 - z_2^2)}\right) \\ \alpha_1 &= \dot{x}_{1d} - k_1 z_1 \end{aligned} \tag{36}$$

The system parameters of manipulator are: $m = 0.01$ kg $\cdot$m ^{2}, $L = 0.05$H, $R = 2.5\Omega$, $K_i = 1.\ 75$N$\cdot$m/A,

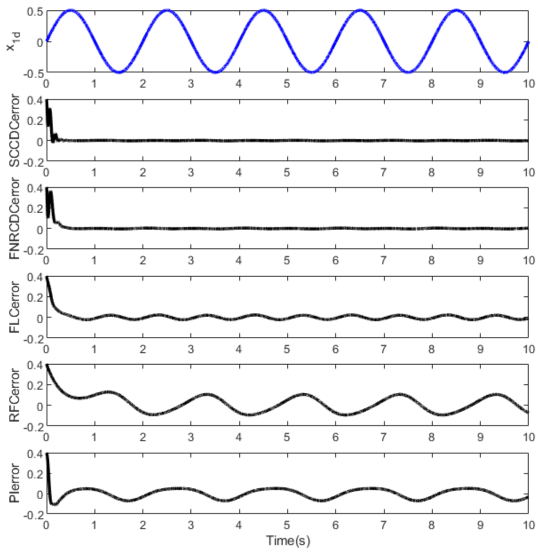

FIGURE 8. The desired trajectory x_{1d} and tracking error.

$K_u = 2$, $K_R = 1$V·s/rad, $b = 0.1$N·m·s/rad. The disturbance $f_d(t) = 0.15\ \sin(t)$N·m. The desired trajectory $x_{1d} = 0.5\sin(\pi t)$, and $x_1(0) = 0.4$, $x_2(0) = 0$. The following five controllers are applied to test the validity of the proposed controller:

Remark 6: When the initial state of the system is not matched, the control system produces a large initial acceleration and initial velocity. It can be seen whether the controller can restrain all the states of the system and verify the effectiveness of the control strategy, so the initial values of the state $x_1(0)$ is set to be 0.4.

SCCDC: The state constraint controller with disturbance compensation proposed in Section III of this paper. The control parameters are selected as $k_1 = 20$, $k_2 = 30$, $k_3 = 30$, $b_1 = 0.05$, $b_2 = 0.6$, $b_3 = 10$, $L_1 = 1$, $L_2 = 20$, $L_3 = 25$. The observer gains are $\omega_1 = 150$, $\omega_2 = 100$.

FNRCDC: The feedback nonlinear robust controller with disturbance compensation, the controller is given as $u = \frac{1}{1+x_1^2}\left[-0.1x_1x_2 + 0.2x_2 - \hat{x}_{e2} + \dot{\alpha}_{1c} - k_2z_2\right]$, where $\dot{\alpha}_{1c} = \frac{\partial\alpha_1}{\partial t} + \frac{\partial\alpha_1}{\partial x_1}\dot{\hat{x}}_1 + \frac{\partial\alpha_2}{\partial\hat{x}_{e1}}\dot{\hat{x}}_{e1}$, $\alpha_1 = -0.1x_1^2 - \hat{x}_{e1} + \dot{x}_{1d} - k_1z_1$. The controller gains are given as $k_1 = 20$, $k_2 = 30$, $k_3 = 30$, $\omega_1 = 150$, $\omega_2 = 100$.

FLC: The feedback linearization controller without disturbance compensation. The controller gains are given as $k_1 = 20$, $k_2 = 30$, $k_3 = 30$.

RFC: The robust feedback controller only with the linear robust feedback term and without disturbance compensation and model compensation term, the controller is given as $u = -k_1\dot{z}_1 - k_2z_2$, the feedback gains are selected same as corresponding feedback gains of the FNRCDC controller.

PI: This is the proportional-integral-derivative controller; it is also widely utilized in industries The P-gain, I-gain are tuned to be $k_p = 9.526$, $k_i = 41.65$ by PID tuner.

Fig.8 shows the system tracking performance of five controllers and the best tracking performance is achieved by SCCDC (the tracking error is about 2.4×10^{-3}, the tracking errors of FNRCDC, FLC, RFC and PI are about 4.45×10^{-3} , 2.35×10^{-2}, 0.105 and 0.05, respectively) . The state estimations and estimation errors of x_1, x_2 and x_3 in SCCDC and FNRCDC are given in Fig.9, Fig.10 and Fig.11, respectively. As seen, even with big estimation errors caused by the unmatched system initial state, the system steady-state

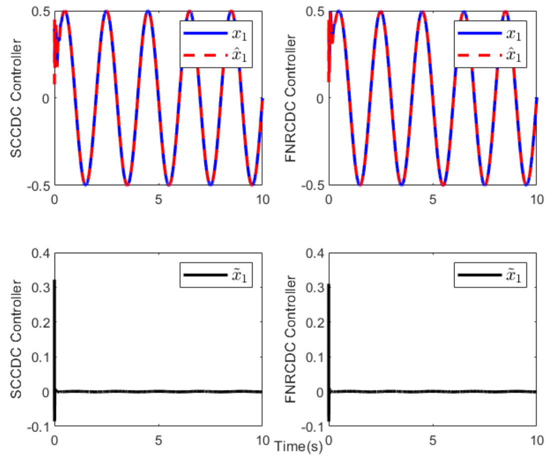

FIGURE 9. x_1, estimation of x_1 and estimation error.

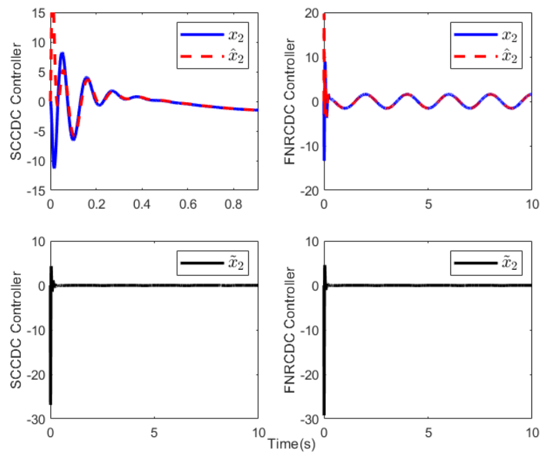

FIGURE 10. x_2, estimation of x_2 and estimation error.

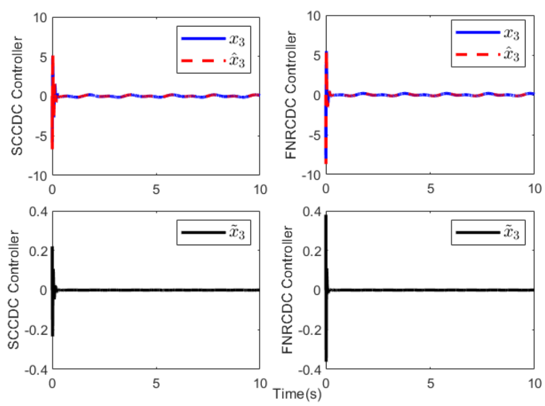

FIGURE 11. x_3, estimation of x_3 and estimation error.

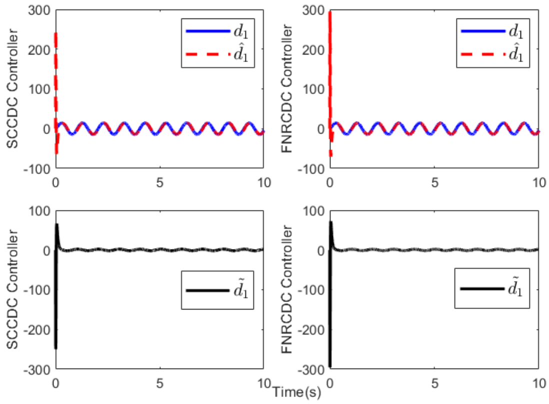

FIGURE 12. d_1, x_{e2} and estimation error.

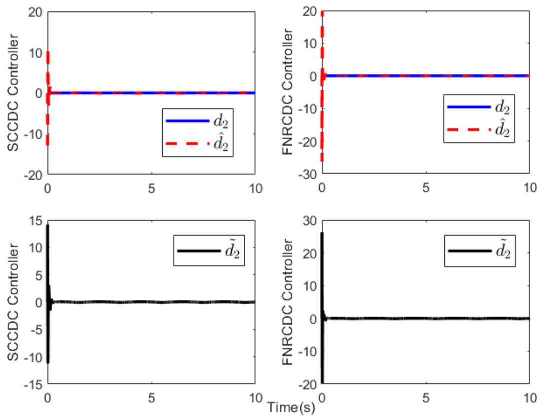

FIGURE 13. The graph of x_{e3}.

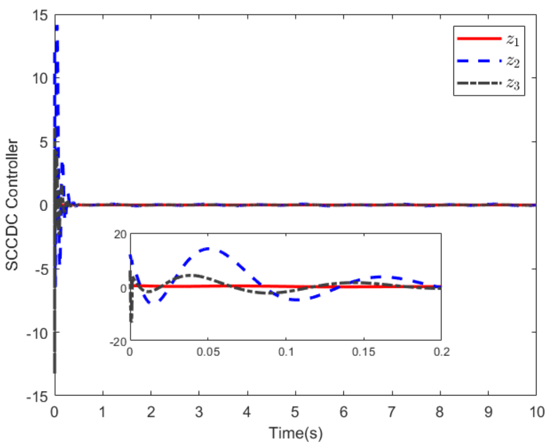

FIGURE 14. The graph of z_1, z_2 and z_3.

estimations are accurate. Fig.12 presents d_1, x_{e2} and estimation errors of SCCDC and FNRCDC; Fig.13 presents d_2, x_{e3} and estimation errors of SCCDC and FNRCDC. From the two figures, it is obvious that the actual disturbance estimation is obtained by ESO. The z_1, z_2 and z_3 are illustrated in Fig.14. From this figure, it can be obvious that the bounds for z_1, z_2 and z_3 are not overstepped. Fig.15 shows the x_1, x_2 and x_3 of SCCDC and FNRCDC, we can see that the full state

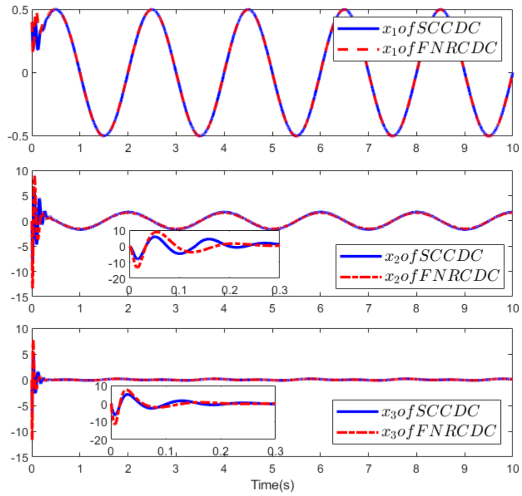

FIGURE 15. x_1, x_2 and x_3 of SCCDC Controller and FNRCDC Controller.

constraints are not overstepped in SCCDC and the state constraints are overstepped in FNRCDC. The effectiveness of the proposed control strategy is further illustrated.

V. CONCLUSION

In this study, a state constraint controller for a class of nonlinear systems with disturbances and full state constraints is proposed. Based on BLFs, a backstepping design with ESO is constructed, and then it is proved that all the signals are bounded in the closed-loop system with no violation of the full state constraints. Finally, two simulation examples are given to illustrate the performance of the proposed approach.

REFERENCES

[1] N. Bekiaris-Liberis and M. Krstic, "Stability of predictor-based feedback for nonlinear systems with distributed input delay," *Automatica*, vol. 70, pp. 195–203, Aug. 2016.

[2] J. Gong and B. Yao, "Neural network adaptive robust control of nonlinear systems in semi-strict feedback form," *Automatica*, vol. 37, no. 8, pp. 1149–1160, 2001.

[3] J. Yao, W. Deng, and Z. Jiao, "Adaptive control of hydraulic actuators with LuGre model-based friction compensation," *IEEE Trans. Ind. Electron.*, vol. 62, no. 10, pp. 6469–6477, Oct. 2015.

[4] A. Levant, "Sliding order and sliding accuracy in sliding mode control," *Int. J. Control*, vol. 58, no. 6, pp. 1247–1263, 1993.

[5] Y. Shtessel, M. Taleb, and F. Plestan, "A novel adaptive-gain supertwisting sliding mode controller: Methodology and application," *Automatica*, vol. 48, no. 5, pp. 759–769, 2012.

[6] S. Yu, X. Yu, B. Shirinzadeh, and Z. Man, "Continuous finite-time control for robotic manipulators with terminal sliding mode," *Automatica*, vol. 41, no. 11, pp. 1957–1964, Nov. 2005.

[7] Z. Yao, J. Yao, and W. Sun, "Adaptive RISE control of hydraulic systems with multilayer neural-networks," *IEEE Trans. Ind. Electron.*, vol. 66, no. 11, pp. 8638–8647, Nov. 2019.

[8] S. Li, J. Yang, W. Chen, and X. Chen, *Disturbance Observer-Based Control: Methods and Applications*. Boca Raton, FL, USA: CRC Press, 2014.

[9] J. Yao and W. Deng, "Active disturbance rejection adaptive control of uncertain nonlinear systems: Theory and application," *Nonlinear Dyn.*, vol. 89, no. 3, pp. 1611–1624, May 2017.

[10] Q.-C. Zhong and D. Rees, "Control of uncertain LTI systems based on an uncertainty and disturbance estimator," *J. Dyn. Syst., Meas., Control*, vol. 126, no. 4, pp. 905–910, 2004.

[11] W.-H. Chen, "Disturbance observer based control for nonlinear systems," *IEEE/ASME Trans. Mechatronics*, vol. 9, no. 4, pp. 706–710, Dec. 2004.

[12] H. Gritli and S. Belghith, "Robust feedback control of the underactuated inertia wheel inverted pendulum under parametric uncertainties and subject to external disturbances: LMI formulation," *J. Franklin Inst.*, vol. 355, no. 18, pp. 9150–9191, 2018.
[13] J. Davila, "Exact tracking using backstepping control design and high-order sliding modes," *IEEE Trans. Autom. Control*, vol. 58, no. 8, pp. 2077–2081, Aug. 2013.
[14] L. Shi, C. K. Ahn, and Z. Xiang, "Adaptive fuzzy control of switched nonlinear time-varying delay systems with prescribed performance and unmodeled dynamics," *Fuzzy Sets Syst.*, vol. 371, pp. 40–60, Sep. 2019.
[15] Y. Dong and B. Ren, "UDE-based variable impedance control of uncertain robot systems," *IEEE Trans. Syst., Man, Cybern., Syst.*, to be published. doi: 10.1109/TSMC.2017.2767566.
[16] J. Han, "A class of extended state observers for uncertain systems," (in Chinese), *Control Decis.*, vol. 10, no. 1, pp. 85–88, 1995.
[17] H. Pan, W. Sun, H. Gao, T. Hayat, and F. Alsaadi, "Nonlinear tracking control based on extended state observer for vehicle active suspensions with performance constraints," *Mechatronics*, vol. 30, pp. 363–370, Sep. 2015.
[18] J. Yao and W. Deng, "Active disturbance rejection adaptive control of hydraulic servo systems," *IEEE Trans. Ind. Electron.*, vol. 64, no. 10, pp. 8023–8032, Oct. 2017.
[19] R. Cui, L. Chen, C. Yang, and M. Chen, "Extended state observer-based integral sliding mode control for an underwater robot with unknown disturbances and uncertain nonlinearities," *IEEE Trans. Ind. Electron.*, vol. 64, no. 8, pp. 6785–6795, Aug. 2017.
[20] H. Xing, J. H. Jeon, K. C. Park, and I. K. Oh, "Active disturbance rejection control for precise position tracking of ionic polymer–metal composite actuators," *IEEE/ASME Trans. Mechatronics*, vol. 18, no. 1, pp. 86–95, Feb. 2013.
[21] R. J. Liu, M. Wu, G. P. Liu, J. She, and C. Thomas, "Active disturbance rejection control based on an improved equivalent-input-disturbance approach," *IEEE/ASME Trans. Mechatronics*, vol. 18, no. 4, pp. 1410–1413, Aug. 2013.
[22] H. An, H. Xia, and C. Wang, "Barrier Lyapunov function-based adaptive control for hypersonic flight vehicles," *Nonlinear Dyn.*, vol. 88, no. 3, pp. 1833–1853, May 2017.
[23] C. Dong, Y. Liu, and Q. Wang, "Barrier Lyapunov function based adaptive finite-time control for hypersonic flight vehicles with state constraints," *ISA Trans.*, to be published. doi: 10.1016/j.isatra.2019.06.011.
[24] K. P. Tee and S. S. Ge, "Control of nonlinear systems with partial state constraints using a barrier Lyapunov function," *Int. J. Control*, vol. 84, no. 12, pp. 2008–2023, 2011.
[25] J. Zhang, G. Li, Y. Li, and X. Dai, "Barrier Lyapunov functions-based localized adaptive neural control for nonlinear systems with state and asymmetric control constraints," *Trans. Inst. Meas. Control*, vol. 41, no. 6, pp. 1656–1664, 2019.
[26] C. Wang, Y. Wu, and J. Yu, "Barrier Lyapunov functions-based dynamic surface control for pure-feedback systems with full state constraints," *IET Control Theory Appl.*, vol. 11, no. 4, pp. 524–530, Mar. 2017.
[27] Y.-J. Liu and S. Tong, "Barrier Lyapunov functions-based adaptive control for a class of nonlinear pure-feedback systems with full state constraints," *Automatica*, vol. 64, pp. 70–75, Feb. 2016.
[28] C. Wang and Y. Wu, "Finite-time tracking control for strict-feedback nonlinear systems with full state constraints," *Int. J. Control*, vol. 92, no. 6, pp. 1426–1433, Nov. 2017. doi: 10.1080/00207179.2017.1397290.
[29] T. Zhang, M. Xia, and Y. Yi, "Adaptive neural dynamic surface control of strict-feedback nonlinear systems with full state constraints and unmodeled dynamics," *Automatica*, vol. 81, pp. 232–239, Jul. 2017.
[30] T. Zhang, M. Xia, Y. Yi, and Q. Shen, "Adaptive neural dynamic surface control of pure-feedback nonlinear systems with full state constraints and dynamic uncertainties," *IEEE Trans. Syst., Man, Cybern., Syst.*, vol. 47, no. 8, pp. 2378–2387, Aug. 2017.
[31] W. Liu, Q. Ma, G. Zhuang, J. Lu, and Y. Chu, "An improved adaptive neural dynamic surface control for pure-feedback systems with full state constraints and disturbance," *Appl. Math. Comput.*, vol. 358, pp. 37–50, Oct. 2019.
[32] D. Ye, Y. Cai, H. Yang, and X. Zhao, "Adaptive neural-based control for non-strict feedback systems with full-state constraints and unmodeled dynamics," *Nonlinear Dyn.*, vol. 97, no. 1, pp. 715–732, 2019.
[33] Q. Zheng, L. Gao, and Z. Gao, "On stability analysis of active disturbance rejection control for nonlinear time-varying plants with unknown dynamics," in *Proc. IEEE Conf. Decis. Control*, Dec. 2007, pp. 3501–3506.
[34] Q. Guo, Y. Zhang, B. Celler, and S. Su, "Backstepping control of electro-hydraulic system based on extended-state-observer with plant dynamics largely unknown," *IEEE Trans. Ind. Electron.*, vol. 63, no. 11, pp. 6909–6920, Nov. 2016.
[35] M. Fu, T. Wang, and C. Wang, "Barrier Lyapunov function-based adaptive control of an uncertain hovercraft with position and velocity constraints," *Math. Prob. Eng.*, vol. 2019, pp. 1–16, Feb. 2019, Art. no. 1940784.
[36] J. Li and Q. Zhang, "Fuzzy reduced-order compensator-based stabilization for interconnected descriptor systems via integral sliding modes," *IEEE Trans. Syst., Man, Cybern., Syst.*, vol. 49, no. 4, pp. 752–765, Apr. 2019.
[37] R. Gao, D. Zhai, and J. Cheng, "Decentralized static output feedback sliding mode control for interconnected descriptor systems via linear sliding variable," *Appl. Math. Comput.*, vol. 357, pp. 185–198, Sep. 2019.
[38] B. Ren, S. S. Ge, K. P. Tee, and T. H. Lee, "Adaptive neural control for output feedback nonlinear systems using a barrier Lyapunov function," *IEEE Trans. Neural Netw.*, vol. 21, no. 8, pp. 1339–1345, Aug. 2010.
[39] K. P. Tee, S. S. Ge, and E. H. Tay, "Barrier Lyapunov functions for the control of output-constrained nonlinear systems," *Automatica*, vol. 45, no. 4, pp. 918–927, Apr. 2009.

ZHANGBAO XU was born in Anhui, China, in 1988. He received the B.S. degree in mechanical engineering and automation from Huaqiao University, Xiamen, China, in 2012, and the Ph.D. degree in mechanical engineering from the Nanjing University of Science and Technology, Nanjing, China, in 2017. In 2017, he joined as a Lecturer with the School of Mechanical Engineering, Anhui University of Technology, Ma'anshan, China. His current research interests include the high accuracy servo control of mechatronic systems, adaptive, and robust control.

LAN LI received the master's degree in mechatronics from Beihang University, Beijing, China, in 2008. She joined the China Academy of Launch Vehicle Technology, Beijing, where she is currently a Senior Engineer. Her current research interests include general design and the servo control techniques of vehicle systems.

JIANYONG YAO was born in Shandong, China, in 1984. He received the B.Tech. degree from Tianjin University, Tianjin, China, in 2006, and the Ph.D. degree in mechatronics from Beihang University, Bejing, China, in 2012. In 2012, he joined the School of Mechanical Engineering, Nanjing University of Science and Technology, Nanjing, China, where he is currently a Professor. His current research interests include the high accuracy servo control of mechatronic systems, adaptive and robust control, fault detection, and the accommodation of dynamic systems.

XIAOLEI HU was born in Anhui, China, in 1987. He received the B.S. degree from Anhui Agricultural University, Hefei, China, in 2009, and the Ph.D. degree in mechanical engineering from the Nanjing University of Science and Technology, Nanjing, China, in 2015. In 2016, he joined the School of Mechanical Engineering, Anhui University of Technology, Ma'anshan, China, where he is currently a Lecturer. His current research interests include flow field analysis and dynamic analysis.

QINGYUN LIU was born in Shandong, China, in 1973. He received the B.S. degree from the Anhui Industry Institute, Hefei, China, in 1996, and the M.S. and Ph.D. degrees in mechanical engineering from Southeast University, Nanjing, China, in 2003 and 2007, respectively. In 2007, he joined the School of Mechanical Engineering, Anhui University of Technology, Ma'anshan, China, where he is currently a Professor. His current research interests include robotics and industrial automation.

NENGGANG XIE received the B.S. degree from the Harbin Institute of Shipbuilding Engineering, Harbin, China, in 1993, and the M.S. and Ph.D. degrees in civil engineering from Hohai University, Nanjing, China, in 1996 and 1999, respectively. In 1999, he joined the School of Mechanical Engineering, Anhui University of Technology, Ma'anshan, China, where he is currently a Professor. His current research interests include computational mechanics, optimization, and control.